Pharmacokinetics of Chemopreventive Compounds

by

RACHEL TSAI-HAN WU

A Thesis submitted to the

Graduate School-New Brunswick

Rutgers, The State University of New Jersey

in partial fulfillment of the requirements

for the degree of

Master of Science

Graduate Program in Pharmaceutical Sciences

written under the direction of

Dr. Tony Ah-Ng Kong

and approved by

_____

_____

_____

New Brunswick, New Jersey

October, 2008

ABSTRACT OF THE THESIS

Pharmacokinetics of Chemopreventive Compounds

By RACHEL T. WU

Thesis Director:
Dr. Tony Ah-Ng Kong

Cancer claims millions of lives per year. In an effort to find cures to cancer, scientists have turned to chemopreventive compounds that are ingested by humans on a daily basis. Butylated hydroxyanisole (BHA) is a synthetic phenolic antioxidant that is commonly used as a food preservative. Previous studies done on BHA have shown it to exhibit a wide range of biological activities that include protection against acute toxicity of chemicals, modulation of macromolecule synthesis and immune response, induction of phase II detoxifying enzymes, and its potential tumor-promoting activities. Other studies have shown it to have chemopreventive effects. However, little is known about the pharmacokinetics of BHA. The first part of this thesis proposes a study to understand the pharmacokinetics of BHA better. The data showed that BHA followed linear pharmacokinetics within the tested intravenous doses of 10 and 25 mg/kg. The volume of distribution was found to be 1.8 L/kg with a plasma clearance of 60 mL/min/kg and a half-life of 0.7 hr. The bioavailability of BHA at oral doses of 25 mg/kg and 200 mg/kg was found to be 33% and 6%, respectively. The second part of this thesis investigates the effect that Nuclear E2-factor related factor 2 (Nrf2) has on the pharmacokinetics of BHA. Nrf2 belongs to the Cap'n'Collar family of basic region-leucine zipper transcription factors, has been shown to be an essential component of ARE-binding transcriptional

machinery. Nrf2 is thought to facilitate the induction of many phase II detoxifying genes. The results of this study showed that Nrf2 deficient mouse had more extended and greater exposure to BHA when the compound is given orally than Nrf2 wild type mice. This suggests that Nrf2 gene may be involved in the metabolism of BHA. The third part of this thesis investigates the usage of nanoparticle drug delivery systems. Previous pharmacokinetics studies done on chemopreventive compound, Dibenzoylmethane (DBM), which is a ß-diketone structural analog of curcumin, is a minor constituent of licorice, yield unfavorable results. The bioavailability of DBM when given orally was found to be only 7%. This study was proposed in an effort to increase the bioavailability of DBM. The data showed promising results. When DBM was administered orally to rats in a nanoparticle emulsion, all the pharmacokinetic parameter values increased significantly, compared to the pharmacokinetics parameter values yielded after oral administration of an equal dose in the previous delivery vehicle. The bioavailability increased from 7% to 36% at an oral dose of 250 mg/kg. Similar results were found in a test done on mice.

Acknowledgements:

First off, I would like to thank my thesis advisor, Dr. Tony Kong, whose guidance got me where I am today. The guidance and support that he has shown me during my time at Rutgers University will always be greatly appreciated. I would also like to thank Dr. Tamara Minko and Dr. Renping Zhou for being on my defense committee and giving me valuable insights.

I would like to especially thank my fellow lab member, Ms. Wen Lin, for the support, guidance, and patience she has shown me during my time at Rutgers. In addition, I would thank all of my lab members, Dr. Tin-Oo Khor, Dr. Siwang Yu, Dr. Wenge Li, Dr. Constance Saw, Dr. Auemduan Prawan, Mr. William Ka Lung Cheung, Mr. Tien-Yuan Wu, Mr. Jung-Hwan Kim, and Ms. Avantika Barve for all their help.

Lastly, I would like to thank my parents and siblings for the support they have shown me during my Masters studies.

Dedicated to:

My father, Ming-Hong Wu

My mother, Diane Li-Chun Wu

My oldest brother, Andrew Yu-Bing Wu

My older brother, Michael Yu-Chi Wu

My older sister, Cheryl Tsai-Luen Wu-Nguyen

My nephew, Koi Ting-Yu Nguyen

TABLE OF CONTENTS

List of Tables

List of Figures

Introduction

The war against cancer has been raging on as mankind continuously fight against the disease that contributes to 13% of all deaths, claiming 7.6 million lives in 2007. As technology advances, so have our weapons to battle against cancer. With discovery of radiation therapy or surgery, we have saved many lives from falling into the deadly hands of cancer. Although, these treatments are effective against cancer, they are painful and only effective against killing cancerous cells, not stopping them from spreading. Thus, it is not uncommon for those treated with these treatments to have inflicted with cancer again, because the root of the cancer has not been eradicated, but rather the affected cells were just killed off. Cancer begins on a molecular level, where some sort of mutagen that causes mutations in the cells, affecting their growth and metastasis processes, transforming these cells into cancerous cells that multiply uncontrollably(1). Upon this understanding, humans have sought ways to fight cancer on the molecular level, disturbing the pathways that are thought to transform cells into cancerous ones, thus launching the age of chemotherapy.

With an initiation of chemotherapy, many compounds that are both natural and synthetic were reexamined in a new light. Having been discovered to have potential chemopreventive abilities, these compounds were thoroughly investigated in hopes of finding the molecular explanations for their chemopreventive powers and tested in animals to have a better understanding of their pharmacokinetics properties. Butylated hydroxyanisole (BHA) and Dibenzoylmethane (DBM) are such two compounds that were found to be chemopreventive(2,3). The following series of studies are conducted to shed some knowledge on the pharmacokinetics properties of BHA and DBM.

CHAPTER 1

Pharmacokinetics and Metabolism of Phenolic Chemopreventive Compound Butylated Hydroxyanisole

1.1 Introduction

Butylated hydroxyanisole (BHA) is a synthetic phenolic antioxidant that is commonly used as a food preservative. It also exhibits a wide range of biological activities that include protection against acute toxicity of chemicals, modulation of macromolecule synthesis and immune response, induction of phase II detoxifying enzymes, and its potential tumor-promoting activities (4). Numerous animal model studies have shown that phenolic compounds with the inclusion of BHA are efficient chemopreventive agents against carcinogensis, induced by known carcinogens in a range of organ and tissue sites. The chemopreventive effect of BHA is presumed to occur through the induction of many phase II detoxifying enzymes that include glutathione *S*-transferases (GSTs) and UDP-glucuronosyltransferases (UGT) and the inhibition of cytochrome P-450 monooxygenase(5,6). On the down side, other studies have found BHA to be toxic, possibly carcinogenic, in high doses. A study using rodent models showed that excessive BHA causes carcinoma formation in the fore stomachs of the animals (7,8). In previous studies done in our lab, we have observed that BHA displayed a dose-dependent toxic effect (in high dose) in human hepatoma HepG2 cells, human cervical squamous carcinoma HeLa cells, and rat hepatocytes (2,9).

As BHA's biological activities are continuously defined and modified and the possible mechanisms that it may work through that accounts for its chemopreventive

effects are being investigated and elucidated, very limited studies have been done to examine the pharmacokinetics of BHA, which are integral to the development of BHA into a potential chemopreventive agent. In this study, we evaluate the *in vivo* pharmacokinetics of BHA in rats, following intravenous and oral administrations.

1.2 Pharmacokinetics of BHA in the rats

1.2.1 Materials and Methods

1.2.1.1 Animals and Dosing: Male Sprague-Dawley rats weighing 250-300 grams, implanted with a jugular vein cannuale were ordered from Hilltop Laboratory Animals (Scottdale, PA). The rats were housed at the Animal Care Facility of Rutgers University, where they were acclimatized for three days with free access to food and water. Rats were fasted overnight and given doses of BHA at 25 and 200 mg/kg in a vehicle of Cremaphor EL/tween-80/ethanol/water (1:1:1:7) via oral gavage. A second group of rats were given BHA in 10 and 25 mg/kg intravenous route through the jugular vein cannulae via the same vehicle. After administration of BHA, 300 μL blood samples were collected at subsequent time points of 2 (i.v. only), 5, 15, 30 min, 1, 1.5, 2, 4, 6, 12, and 24h. The plasma was separated by centrifugation and stored at -80^{o}C until further analysis.

1.2.1.2 Chemicals and reagents: Butylated Hydroxyanisole (BHA) and internal standard 3-methoxylphenol were purchased from Sigma (St. Louis, MO, USA) at purity of more than 98%. Acetonitrile and methanol were all HPLC grade from Fisher Scientific. Formic acid (FA) was spectrophotometric grade (>99%, Aldrich, WI, USA).

Ethyl acetate was purchased from Sigma with purity of 99.9%. Other chemicals used in the study were all in analytic grade unless specified.

1.2.1.3 HPLC Assay: HPLC analysis was performed on the collected plasma samples to measure their respective concentration of BHA. The Shimadzu HPLC system (SCL-10A vp) consists a model FVC-10AL vp binary pump, a model SIL-10AD vp autosampler (a 250 µL injector and a 100 µL loop) configured with a 4°C cooler, and a model SPD-10AV vp UV-Vis detector. The column and autosampler temperatures were kept at room temperature and 4°C, respectively. The reverse phase column (Gemini™ C18 column, 150 x 2.0 mm, 5-µm, Phenomenex, Torrance, CA USA) with a SecurityGuard™ cartridge system (Phenomenex) were used in the analysis. The gradient was modified from a method used in a previous study (10). The gradient mobile phases were pumped through the system at a flow rate of 0.2 mL/min. Original conditions of the gradient used in this study were 90% of 5 mM ammonium with 0.1% formic acid acetate mobile phase A and 10% of methanol/water (98:2 v/v) with 0.1% formic acid mobile phase B. Between 0 and 15 minutes, the percentage of mobile phase B was increased linearly from 10% to 100%. Between 15 and 23 minutes, mobile phase B was maintained at 100%. Between 23 and 25 minutes, the percentage of mobile phase B was decreased to 10% and mobile phase A was increased to 90%. From 25 to 35 minutes, the mobile phase A was held at 90% and B at 10%. The flow rate was 0.2 mL/min and the injection volume was 50 µL. The UV detector was set at a single wavelength of 280 nm. The Class-VP software version 7.1.1 (Shimadzu, MD USA) was used for the instrument control and data analysis. The retention times for BHA and its internal standard are 21.5 and 16 minutes, respectively.

1.2.1.4 Samples preparation procedures: A 100 µL blank, spiked plasma or pharmacokinetics study plasma sample was spiked with extracted with the internal standard working solution. It was then extracted twice with 400 followed by 200 µL of ethyl acetate/methanol/acetic acid (94.75/4.75/0.5 v:v) solution. With each extraction, the plasma was mixed for 4 min on a cyclomix with the extraction solution followed by centrifugation at 10,000 g for 3 min. The upper organic layer was removed after centrifugation and transferred into a separate tube and evaporated under nitrogen gas at room temperature. The residual substance was reconstituted in 100 µL of acetonitrile/water (50:50 v/v) by vortexing for 4 min; the reconstituted sample was filtered by a 0.45 µm Nylon Spin-filter (Analytic Sales, NJ USA) and transferred into a sample vial for HPLC analysis.

1.2.1.5 Pharmacokinetics Analysis: The pharmacokinetic parameters of BHA were obtained by analyzing the BHA plasma concentration data by non-compartmental means using WinNonlin 4.0 software (Pharsight, CA USA). The area under the plasma concentration versus time (AUC_{0-t}) from time zero to time of the last measured concentration (C_{last}) was calculated using the log-linear trapezoidal rule. The slope of (k_{el}) of the terminal phase of concentration-time profile was determined by the log-linear regression of a minimum of three data points. Following i.v. dosing, total clearance (CL) was calculated by dividing the administered dose by the calculated AUC. The mean residence time was calculated by dividing the area under the first moment curve (AUMC) by AUC, as follows: $MRT=AUMC_{0\rightarrow\infty}/AUC_{0\rightarrow\infty}$. The volume of distribution at steady state (V_{ss}) is then calculated using CL and MRT, as follows: $V_{ss}=CL \bullet MRT$. The absorption rate (*ka*) is calculated by equation: $MRT_{PO} - MRT_{IV} = 1/ka$.

1.2.1.6 Blood to plasma partitioning ratio analysis: The blood to plasma partitioning ratio (C_B/C_p) for BHA was done in fresh, pooled rat blood (Bioreclamation Inc.) BHA in stock solutions of 25, 100 and 1000 µg/mL in methanol was added into 500 µL of blood at a ratio of 1:100 to give a final concentration of 0.25 µg/mL, 1 µg/mL, and 10 µg/mL, respectively. Samples were incubated at 37^{o}C in water bath for one hour. The plasma was separated immediately by centrifugation and analyzed by HPLC-UV detection. Each concentration was done in sets of triplicates.

1.2.1.7 Protein Binding Analysis: The extent of plasma protein binding of BHA was determined at 37^{o}C using an ultrafiltration method. Briefly, BHA in stock solutions of 0.100, 1, 5, and 25 mg/mL was added into 50 µL of blank plasma (Hilltop Animals, PA USA). The plasma was then mixed for 30 sec and incubate at 37^{o}C for 30 min. The minxture was transferred in a micropartition device (Millipore, Bedford, MA) followed by centriguation at 2000 g for 30 min to generate ultrafiltration. The unbound fraction in plasma was determined from the ratio of ultrafiltrate to plasma concentration. Each concentration was done in sets of triplicates.

1.2.1.8 Statistical Analysis: Statistical analysis was conducted using the student's T-test. Statistical significance was set at $p \leq 0.05$.

1.2.2 Results and Discussion

The food preservative BHA is thought to have chemopreventive effects. A number of studies have been dedicated to initially the validation of BHA as a chemopreventive agent and currently the molecular mechanisms and signal pathways that BHA affects are being proposed and looked into. Increased interest in BHA calls for a

further investigation into its basic properties, such as its pharmacokinetics properties. This study sets out to examine certain pharmacokinetics properties of BHA that may be helpful for further exploration of BHA as a potential chemopreventive agent.

The plasma clearance of BHA was 68.08 ± 13.99 and 59.58 ± 7.37 mL/min/kg following i.v. doses of 10 and 25 mg/kg, respectively, averaging 63.83 mL/min/kg. The renal clearance of BHA was calculated to be 12.326 mL/min/kg (data not shown). The hepatic clearance of the BHA is then found to be 51.5 mL/min/kg. The blood-to-plasma ratio (C_B/C_p) of BHA in the rats was calculated to be 2.13 ± 0.33, 2.53 ± 1.162 and 2.24 ± .505 for BHA concentrations of 0.25 μg/mL, 1 μg/mL and 10 μg/mL, respectively after being incubated in the blood at 37^{o}C for an hour. These results indicate that the amount of BHA in the blood is around 2.5 times greater than that in the plasma. BHA does not appear to be equally distributed between the plasma and blood cells in rats. The total body clearance from blood was found to be 30.39 mL/min/kg and 26.60 mL/min/kg at an i.v. dose of 10 and 25 mg/kg, respectively, using the blood-to-plasma ratio at the BHA concentration of 10 μg/mL, calculated from an equation used in a previous study (11). The total body clearance from blood of BHA corresponds to 55 % of the hepatic blood flow of 55 ml/min/kg, revealing a moderate clearance. Using literature values of hepatic blood flow, (Q_H, about 55-80 mL/min/kg), the hepatic extraction ratio was found to be range of 0.38 to 0.56, indicating that BHA is a high clearance drug with a decent extraction through the liver in rats (12).

Following intravenous administration of BHA at doses of 10 mg/kg and 25 mg/kg, the $AUC_{0\rightarrow\infty}$ values were 2.52 ± 0.46 and 7.08 ± 0.92 μg•hr/mL, respectively. The dose-normalized plasma concentration-time profiles are superimposable, which

suggests that BHA follows linear pharmacokinetics within the dose range given to the male rats. The values of dose-normalized AUC were 0.252 and 0.283 at doses of 10 and 25 mg/Kg, which are not significantly different, which again suggest linear pharmacokinetics between the two doses. The systemic clearance of BHA in male rats following intravenous injection of 10 and 25 mg/kg were 68.08 ± 13.99 and 59.58 ± 7.37 mL/min/kg, respectively. The $t_{1/2}$ was found to be 0.686 ± 0.064 and 0.727 ± 0.0619 h for doses of 10 mg/kg and 25 mg/kg, respectively. These corresponding values of these two pharmacokinetic parameters were not found to be significantly different between the two doses, using the student's T-test with the p set at $\leq .05$. The plasma clearance and $t_{1/2}$ remaining relatively unchanged between the two i.v. doses further suggest that BHA exhibits linear pharmacokinetics when given intravenously. The volume of distribution at steady state of BHA at 10 and 25 mg/kg was 1.831 ± 0.427 and 1.373 ± 0.399 L, respectively. Both values are greater than the total body water of rats, which is 0.67 L/kg, indicating that BHA may be widely distributed in tissues. BHA's log P value is estimated to be as high as 3.50 (6). The strong liphophilic nature of BHA may account for its wide distribution in tissues. The MRT values of BHA after an i.v. dose of 10 mg/kg was found to be 0.46 ± 0.019 h, which is comparable to the MRT value of 0.38 ± 0.072 h at a dose of 25 mg/kg. The comparability of many of its pharmacokinetic parameters demonstrates BHA's linear pharmacokinetics within the range of the doses tested.

The plasma protein binding analysis yielded results that showed the percentage of free BHA to be 2.31 ± 0.38, 6.69 ± 0.60, 7.67 ± 0.66, 11.12 ± 0.26 at concentrations of 10, 100, 500, and 2500 μg/mL, respectively. These findings suggest that BHA is a highly plasma protein bound compound. Increase in the percentage of unbound compound at

higher doses indicates that the plasma protein binding sites are being oversaturated and are no longer able to bind any more BHA molecules.

Following oral dosing of BHA at 25 and 200 mg/kg, BHA reached C_{max} of 0.90 ± 0.30 and 1.79 ± 0.82 μg/mL at T_{max} of 0.375 ± 0.144 and 1.0625 ± 0.718 h, respectively. The $AUC_{0\rightarrow\infty}$ values for doses of 25 and 200 mg/kg were 2.386 ± 0.414 and 3.54 ± 0.82 μg/mL•h. BHA does not show proportionality or linearity between increase in C_{max} and $AUC_{0\rightarrow\infty}$ with increase dose, suggesting that it may be an absorption-limited compound at higher does. Previous studies showed that BHA is rapidly absorbed in the gastrointestinal tract and metabolized by the liver. The nonlinear relationship between $AUC_{0\rightarrow\infty}$ and dosage may be due in part to the saturation of uptake transport systems in gastrointestinal tract at the higher oral dose, causing BHA to be absorbed slower, accounting for the higher T_{max} at 200 mg/kg. Based on the data from oral and i.v administrations of 25 mg/Kg, absorption rate constant *ka* was calculated to be 0.41 h^{-1}. This value indicates that the absorption rate of BHA is rather rapid with the current emulsion vehicle. !

Absolute bioavailability (F) of BHA was calculated to be 33.48 and 6.32% at does of 25 and 200 mg/kg, respectively. The bioavailability of BHA decreased as the dose increased, which may be a result of the transport system being saturated at the higher dose. Overall, BHA exhibits decent bioavailability at the lower dose, but its bioavailability drops significantly at the higher dose. An interesting phenomenon that is observed in the pharmacokinetics profiles of the rats after an oral administration of 200 mg/kg was that the profiles of two of the rats showed a secondary peak after the first

initial peak, suggesting that there was enterohepatic recirculation of the BHA after oral administration (13).

In conclusion, the data supports the hypothesis that BHA demonstrates linear pharmacokinetics in rats within the range of intravenous doses tested, i.e. 10 to 25 mg/kg. BHA is a highly extracted compound, whose bioavailability varies with the dosage. The data suggests that BHA has great exposure at lower doses than higher doses, proportionally, implicating that a lower dosage of BHA may be as effective as a higher dosage. BHA was found to be a highly absorbed and cleared compound with a short half-life of less than an hour in rats. BHA is susceptible to both hepatic and renal clearance. Reported to having a hormetic effect, BHA needs further investigation to evaluate its usefulness as a chemopreventive compound and find the proper dosage that will yield therapeutic effects.

Table 1.1 Pharmacokinetics parameters of BHA after intravenous administration determined by Noncompartmental Analysis. $N = 4$.

Dose (mg/Kg)	10 ($n = 4$)	25 ($n = 4$)
AUC (μg•hr/mL)	2.52 ± 0.461	7.08 ± 0.918
$T_{1/2}$ (hr)	0.636 ± 0.0647	0.727 ± 0.0619
Cl (mL/min/Kg)	68.08 ± 13.99	59.58 ± 7.37
V_{SS} (L/Kg)	1.831 ± 0.426	1.373 ± 0.399
MRT (hr)	0.461 ± 0.0185	0.379 ± 0.0718
AUC/Dose	0.252	0.283

Table 1.2 Pharmacokinetics parameters of BHA after oral administration determined by Noncompartmental Analysis.

Dose (mg/Kg)	25($n = 4$)	200 ($n = 4$)
AUC (μg•hr/mL)	2.39 ± 0.41	3.58 ± 0.82
T_{max} (hr)	0.38± 0.14	1.06 ± 0.72
C_{max} (μg/mL)	0.90 ± 0.30	1.79 ± 0.82
MRT (hr)	2.81 ± 0.22	2.08 ± 0.26
ka (hr^{-1})	0.41	-
F (%)	33.48	6.32

Figure 1.1 Chemical structure of butylated hydroxyanisole

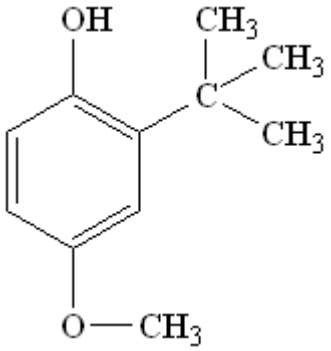

Figure 1.2 The plasma concentration-time profiles of BHA after intravenous administration. Rats were dosed intravenously with 10 or 25 mg/Kg of BHA. Data are expressed as mean ± SD, *n* = 4.

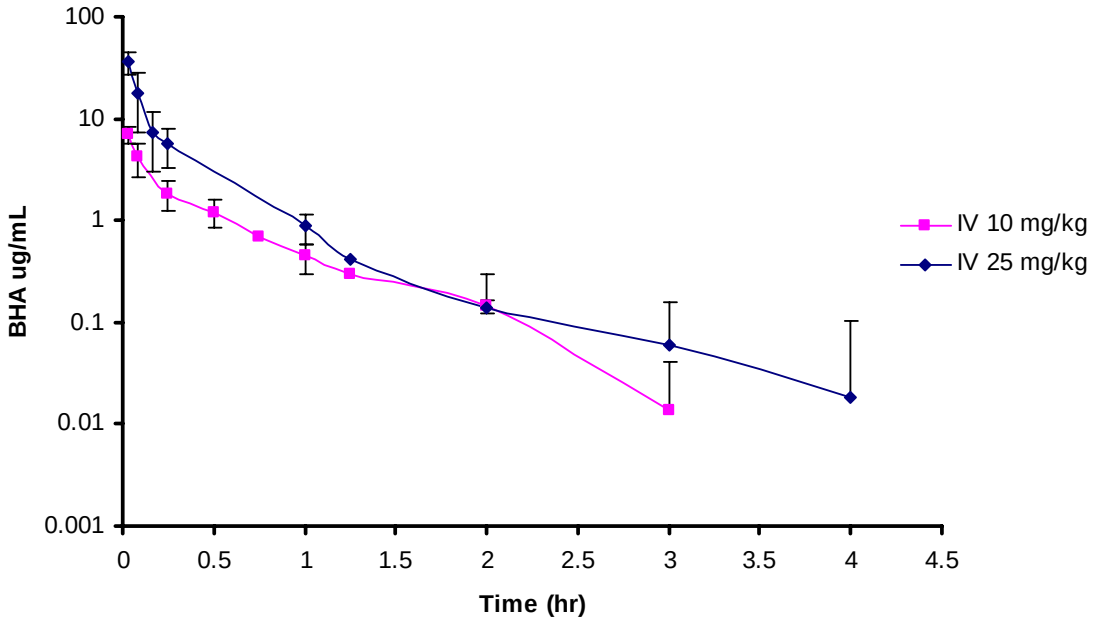

Figure 1.3 The dose normalized plasma concentration-time profiles of BHA after intravenous administration. Rats were dosed intravenously with 10 or 25 mg/Kg of BHA. Data are expressed as mean ± SD, $n = 4$.

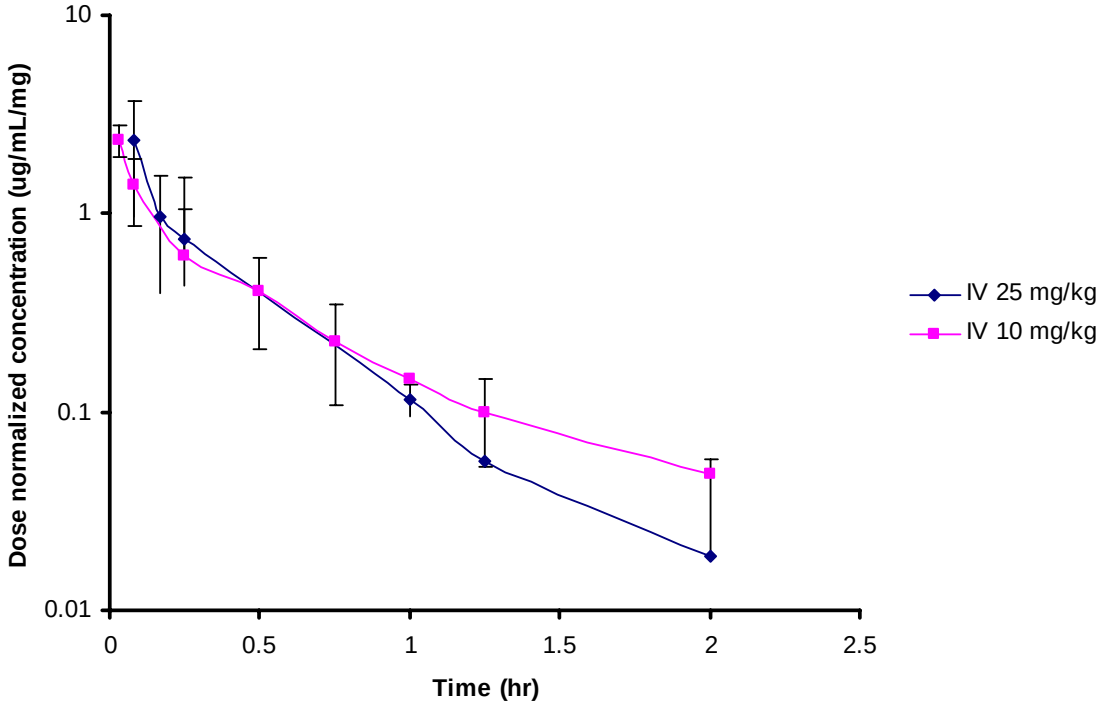

Figure 1.4. The plasma concentration-time profiles of DBM after oral administration. Rats were dosed by oral gavage with 25 and 200 mg/Kg of DBM. Data are expressed as mean ± SD, $n = 4$.

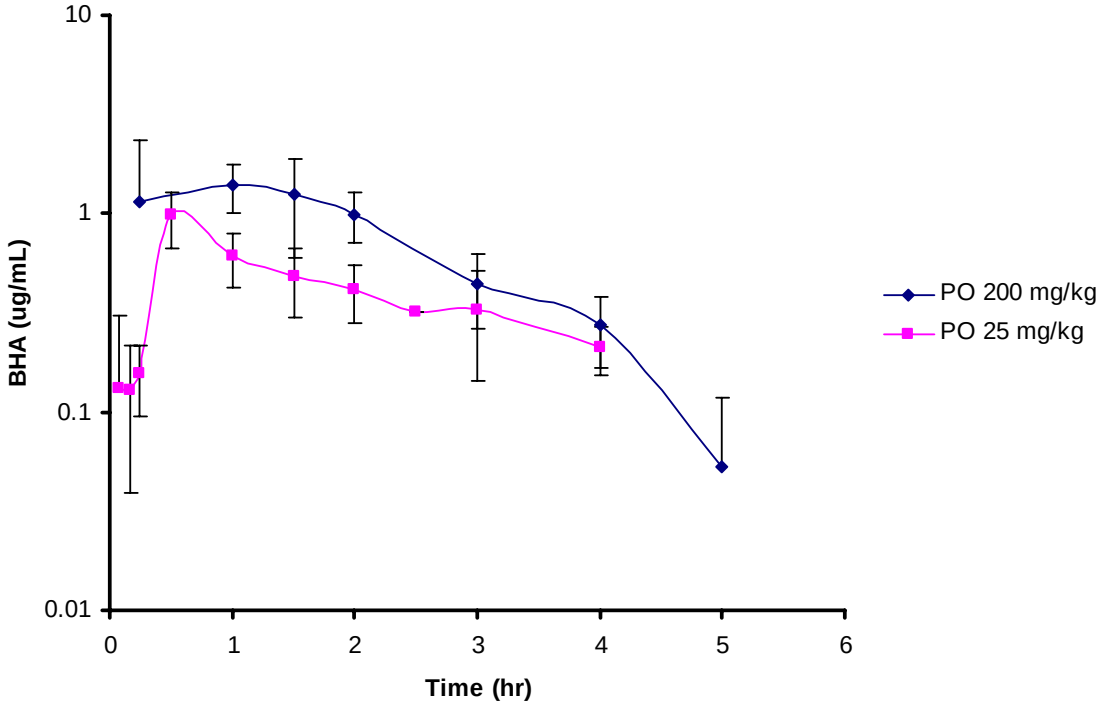

CHAPTER 2

Genetic Impact of Nrf2 Gene on Pharmacokinetics of BHA in C57BL/6J mice

2.1 Introduction:

Phase II detoxifying enzymes, including NAD-(P)H:quinone reductase (NQO1), epoxide hydrolase, γ-glutamylcysteine synthetase (γ-GCS), heme oxygenase-1 (HO-1) and UDP-glycuronosyltransferases, are able to convert reactive electrophiles to less and more easily eliminated compounds, hence shielding cells from a number of chemical stresses and mutagensis and carcinogenesis, thus having chemopreventive effects. Nuclear E2-factor related factor 2 (Nrf2), which belongs to the Cap'n'Collar family of basic region-leucine zipper transcription factors, has been shown to be an essential component of ARE-binding transcriptional machinery (14). Many studies have shown it to play an important role in regulating the expression of many mammalian metabolizing enzymes under oxidative or electrophilic stress with the use of Nrf2-deficient mice (15). These typically regulated enzyme gene expressions were dramatically absent in the Nrf-2 (16). The Nrf2 knockout mice were noted to be more vulnerable to carcinogen-induced carcinogenesis. In previous mice studies we have found that BHA upregulates many metabolizing phase (5,6). These Phase II detoxifying enzymes include, NQO1, γ-GCS, HO-1 and UGT-1A6. It has been demonstrated that regulation of both basal and inducible expression of these phase II metabolizing enzymes is mediated in part by ARE, a *cis*-acting sequence found in the 5′-flanking region of genes encoding many phase II enzymes(17,18). In a previous microarray study, many more of these phase II enzymes that were BHA regulated via the

Nrf2 pathway were identified (6). This study sets out to focus on the connection between pharmacokinetics profiles of both Nrf2 wildtype and deficient mice and their gene expression profiles to further deepen our current understanding BHA and Nrf2-mediated chemoprevention mechanism.

2.2 Materials and Methods

2.2.1 Animals and Dosing: Nrf2(–/–) mice were backcrossed with C57BL/6J wild-type mice (The Jackson Laboratory, Bar Harbor, ME). To confirm the genotype from each animal, DNA was extracted from the tail and analyzed by PCR using the following primers: 3'-primer, 5'-GGAATGGAAAATAGCTCCTGCC-3'; 5'-primer, 5'-GCCTGAGAGCTGTAGGCCC-3'; lacZ primer, 5'-GGGTTTTCCCAGTCACGAC-3'. Nrf2(–/–) and Nrf2(+/+) mice exhibited one band at 200 and 300 bp, respectively (19). The second generation (F2) of male Nrf2 knockout mice was used in this study. C57BL/6J mice were bred and weaned at Rutgers University Animal Facility at Gordon Road. After weaning, C57BL/6J mice were age-matched with F2 Nrf2(–/–) mice (8~12 weeks old), and they were housed Rutgers University Animal Facility under 12 h light/dark cycles with free access to food and water. Groups of 3-4 mice were used for each time point in the pharmacokinetic studies. Before oral dosing, the mice were fasted overnight. They were given BHA at a dose of 200 mg/kg in a vehicle of Cremaphor EL/Tween-80/ethanol/water (1:1:1:7) by oral gavages (p.o). Mice were given an intravenous bolus dose of BHA at a dose of 25 mg/kg in the same vehicle. Blood samples were collected at time point of 2 (i.v. only), 5, 15, 30, 1, 1.5, 2, 4, 6, 8, 12, 24, 36 (p.o. only) h following BHA administration by heart puncture. Plasma was separated immediately by centrifugation and stored at -80^{o}C until analysis.

2.2.2 HPLC Assay: HPLC analysis was performed on the collected plasma samples to measure their respective concentration of BHA. The Shimadzu HPLC system (SCL-10A vp) consists a model FVC-10AL vp binary pump, a model SIL-10AD vp autosampler (a 250 µL injector and a 100 µL loop) configured with a 4°C cooler, and a model SPD-10AV vp UV-Vis detector. The column and autosampler temperatures were kept at room temperature and 4°C, respectively. The reverse phase column (Gemini™ C18 column, 150 x 2.0 mm, 5-µm, Phenomenex, Torrance, CA USA) with a SecurityGuard™ cartridge system (Phenomenex) were used in the analysis. The gradient mobile phases were pumped through the system at a flow rate of 0.2 mL/min. Original conditions of the gradient used in this study were 90% of 5 mM ammonium with 0.1% formic acid acetate mobile phase A and 10% of methanol/water (98:2 v/v) with 0.1% formic acid mobile phase B. Between 0 and 15 minutes, the percentage of mobile phase B was increased linearly from 10% to 100%. Between 15 and 23 minutes, mobile phase B was maintained at 100%. Between 23 and 25 minutes, the percentage of mobile phase B was decreased to 10% and mobile phase A was increased to 90%. From 25 to 35 minutes, the mobile phase A was held at 90% and B at 10%. The flow rate was 0.2 mL/min and the injection volume was 50 µL. The UV detector was set a single wavelength of 280 nm. The Class-VP software version 7.1.1 (Shimadzu, MD USA) was used for the instrument control and data analysis. The retention times for BHA and its internal standard are 21.5 and 16 minutes, respectively.

2.2.3 Samples preparation procedures: A 100 µL blank, spiked plasma or pharmacokinetics study plasma sample was spiked with extracted with the internal standard working solution. It was then extracted twice with 400 followed by 200 µL of

ethyl acetate/methanol/acetic acid (94.75/4.75/0.5 v:v) solution. With each extraction, the plasma was mixed for 4 min on a cyclomix with the extraction solution followed by centrifugation at 10,000 g for 3 min. The upper organic layer was removed after centrifugation and transferred into a separate tube and evaporated under nitrogen gas at room temperature. The residual substance was reconstituted in 100 µL of acetonitrile/water (50:50 v/v) by vortexing for 4 min; the reconstituted sample was filtered by a 0.45 µm Nylon Spin-filter (Analytic Sales, NJ USA) and transferred into a sample vial for HPLC analysis.

2.2.4 Pharmacokinetics Analysis: The pharmacokinetic parameters of BHA were obtained by analyzing the BHA plasma concentration data by non-compartmental means using WinNonlin 4.0 software (Pharsight, CA USA). The area under the plasma concentration versus time (AUC_{0-t}) from time zero to time of the last measured concentration (C_{last}) was calculated using the log-linear trapezoidal rule. The slope of (k_{el}) of the terminal phase of concentration-time profile was determined by the log-linear regression of a minimum of three data points. Following i.v. dosing, total clearance (CL) was calculated by dividing the administered dose by the calculated AUC. The mean residence time was calculated by dividing the area under the first moment curve (AUMC) by AUC, as follows: $MRT=AUMC_{0(\infty}/AUC_{0\rightarrow\infty}$. The volume of distribution at steady state (V_{ss}) is then calculated using CL and MRT, as follows: $V_{ss}=CL \bullet MRT$.

2.3 Results and Discussion

2.3.1 Pharmacokinetics of BHA in wild type C57BL/6J mouse: The pharmacokinetics parameters found after i.v. and oral administration of 25 mg/kg and 200 mg/kg in wild

type mice are summarized in table 2.1 and 2.2. After intravenous (i.v.) administration of BHA at 25 mg/kg, the BHA peaked at a concentration of 35.196 ± 5.45 µg/mL and had a clearance of 25.77 ± 3.36 mL/min/kg, than 50% of the hepatic blood flow of 90 ml/min (20). The V_{ss} was found to be 0.644 ± 0.188 L/kg, which is significantly higher than the average blood volume of mice (0.085 L/kg), suggesting that BHA is widely distributed into the tissues (12). The AUC was found to be 16.36 ± 2.30 µg/mL•hr, which suggests that there is greater exposure of BHA in mice than in rats at the same dose. The absolute bioavailability (F) was calculated by dose-normalized $AUC_{p.o.}/AUC_{i.v.}$ was 39.33%. After oral administration of BHA at 200 mg/kg, the plasma concentration reached its first peak at 5.986 ± 0.314 µg/mL and second one at 10.92 ± 1.44 µg/mL. The first peak was reached almost immediately after administration at 0.139 ± 0.0963 h, suggesting that BHA is absorbed much faster in mice than in Sprague-Dawley rats.

2.3.2 Pharmacokinetics of BHA in Nrf2 knockout mouse: Following i.v. administration of BHA at 25 mg/kg in knockout mice, an interesting phenomenon was observed, the plasma concentration of each corresponding time point was slightly higher in knockout mice than wild type. The highest plasma concentration of BHA in knockout mice (40.49 ± 12.88 µg/mL) was slightly higher than that in wild type (35.196 ± 5.45 µg/mL). The $t_{1/2}$ is 0.378 ± .0802 h, which is very comparable to the $t_{1/2}$ of 0.397 ± .0394 h following i.v. administration at 25 mg/kg in wild type mice. The $t_{1/2}$ in mice is lower than that in rats, which is in conjecture with previous findings that compounds tend to be cleared faster from mice than in rats. The plasma clearance after i.v. administration of 25 mg/kg in knockout mice was found to be 24.71 ± 1.37 mL/kg/min, which is comparable to that of wild type mice. The V_{ss} was found to be 0.706 ± 0.1113 L/kg in knockout

mice, which again suggest wide distribution of BHA into the tissues of the mice. The AUC of the knockout mice after intravenous administration of BHA at 25 mg/kg was calculated to be 16.90 ± 0.957 μg/mL•hr, which is very similar to the AUC found in wild type after i.v. administration of the same dose. Although, the plasma concentrations of BHA after i.v. administration do not differ much, the presence of higher plasma concentration in knockout relative to wild type at several corresponding time points again suggests that BHA may be better absorbed and distributed to the tissues in wild type than in knockout. This phenomenon was not observed following oral administration of BHA at 200 mg/kg in knockout when compared to wild type mice. After oral administration of BHA at 200 mg/kg, the plasma concentration peaked first at 5.098 ± 1.192 and then at 14.24 ± 3.41 μg/mL. The first peak was reached at 0.271 ± 0.172 h. Interestingly, both the first peak concentration and time were lower than those observed in wild type mice. In the first hour after oral administration, every time point concentrations lower in the knockout mice than the respective ones in wild type mice, suggesting that Nrf2 knockout mice might have poor absorption of BHA than wild type mice. However, starting at the 2 hour time point, the plasma concentrations of BHA were higher in the knockout mice than those in the wild type mice at the same sampling points, which suggests that Nrf2 knockout mouse have a slower elimination process for BHA. Dose-normalized $AUC_{p.o.}/AUC_{i.v}$ in knockout mice gave a bioavailability of 58.48%.

2.3.3 Genetic impact of Nrf2 on the pharmacokinetics and metabolism of BHA in C5BL/6J and Nrf2 knockout mice

A comparison between the BHA pharmacokinetics profiles between Nrf2 wild type and knockout mice shows that the initial concentrations of BHA were noticeably lower in the knockout mice after oral administration, which suggests BHA was absorbed to a lesser extent in knockout mice or metabolized faster in Nrf2 knockout mice. In a previous study done, Nrf2 knockout mice were found to have inhibited tolerance to synthetic antioxidants, including BHA. Knockout mice were noted to have lost over 20% of their body weight when fed a 0.5% BHA diet (w/w) over a duration of 13 days while wild type mice under the same regimen gained an average of 1.5% of their body weight, suggesting that BHA is not well absorbed in the knockout mice (15). However, in vitro studies would need to be done to substantiate these findings. Another possible explanation for the initial lower concentrations of BHA in knockout mice may lie in the differential gene expressions between Nrf2 knockout and wild type mice. In a previous microarray study done in our lab that compared that basal gene expression profiles between Nrf2 wild type and knockout mice, we found that the expression of transporter gene (MDR1) was increased by 3.1 and 2.1 fold in the small intestines and liver, respectively in knockout when compared to wild type mice (21). If BHA is a substrate of P-glycoprotein (P-gp), then the increased expression of P-gp might account for the possibility of poorer absorption of BHA in the knockout mice (22). P-gp may cause the absorbed BHA to be exported back into the lumen of the intestines. Being that BHA is a compound that is a rapidly absorbed by the GI tract, the increased expression of P-gp in knockout mice may be the explanation of the lower initial concentrations of BHA

observed in knockout mice. However, given the small molecular weight, BHA might not be a substrate of P-gp.

In previous studies, it was found that BHA was metabolized mainly by cytochrome P450s (9). The elevated levels concentrations of BHA in knockout mice at later time points following oral administration may be explained by the lower expression of these metabolizing enzymes in the liver. However, since microsomal studies were not done, we cannot say that the different concentrations of BHA in knockout and wild type mice are due to the different metabolic abilities of their livers. A more probable explanation for the increase in concentration of BHA and its slower systemic clearance in Nrf2 knockout mice lies within the decreased expression of two major phase II conjugating enzyme gene UDP-glucronyltransferase *UGT2B5* and sulfotransferase *SULT1B1*, which was previously found to be decreased by 2.3 and 2.5 fold in the liver of knockout mice (21). BHA is typically metabolized by cytochrome P450s to *tert*-butylhydroquinone (tBHQ), which is conjugated with glucuronic acid, GSH, or sulfate before elimination from the body (15). The impaired function of these two genes will cause significant accumulation of tBHQ, which may cause the slowdown of the metabolism pathway of BHA and the enzymes involved in it. In addition, in previous studies, we found that NADPH-quinone oxidoreductase was upregulated by BHA via Nrf2 (6). The upregulation of NQO1 may cause tBHQ to be reduced and more water soluble faster in wildtype mice (23). The knockout mice's failure to induce NQO1 in the presence of BHA may also cause the buildup of tBHQ and subsequent the slowing down of the metabolism of BHA. All together, the differential gene expression of phase II conjugating enzymes and transporter genes caused by the removal of the Nrf2 gene in

knockout mice may have altered the pharmacokinetics profile of BHA in mice, which resulted in an overall increased BHA exposure.

2.3.4 Comparison of the pharmacokinetic profiles of BHA in mice and rats: Interestingly, BHA has a lower plasma clearance and greater exposure in mice when compared to rats following both oral and intravenous administration. The $t_{1/2}$ in mice is lower than that in rats, which is in conjecture with previous findings that compounds tend to be eliminated faster from mice than in rats. An interesting observation made in the mice the appearance of a second peak of BHA a few hours after the first initial absorption peak. This secondary peak is more pronounced in the pharmacokinetics profile of the mice than those in rats. The presence of a secondary peak may be due to enterohepatic recirculation (24). The secondary peak in knockout mice was noticeably higher than in wild type. This may be because BHA is less metabolized in the knockout mice, hence why there is more available for recirculation. In addition, the appearance of the secondary peak at a later time in the knockout mice again suggests that BHA is not as well absorbed in knockout mice compared to wild type. Other possibilities for the presence of secondary peaks are presence of absorption windows along the gastrointestinal tract, variations in the condition of the intestinal lumen pH and time-related fluctuations in gastric emptying (13).

Table 2.1 Pharmacokinetics parameters of BHA after intravenous administration determined by Noncompartmental Analysis. Statistics were conducted by ANOVA followed by Bonferroni's test, $n = 3$ or 4.

Dose (25 mg/Kg)	KO ($n = 4$)	WT ($n = 3$)
AUC (μg*hr/mL)	16.90 ± 0.958	16.36 ± 2.30
$t_{1/2}$ (hr)	0.378 ± .0802	0.397 ± .0394
Cl (mL/min/Kg)	24.71 ± 1.37	25.768 ± 3.36
V_{SS} (L/kg)	0.706 ± 0.1113	0.644 ± 0.188
MRT (hr)	0.476 ± 0.0658	0.413 ± .0806

Table 2.2 Pharmacokinetics parameters of BHA after oral administration determined by Noncompartmental Analysis. Statistics were conducted by ANOVA followed by Bonferroni's test, $n = 4$.

Dose (200 mg/Kg)	KO ($n = 4$)	WT ($n = 3$)
AUC (μg*hr/mL)	79.046 ± 3.41	51.49 ± 5.086
t1/2 (hr)	3.18 ± 0.267	1.92 ± 0.19
Tmax (hr)	4.25 ± 0.5	3.33 ± 0.577
C_{max} (μg/mL)	14.237 ± 3.408	10.92 ± 1.44
MRT (hr)	5.90 ± .501	4.28 ± 0.402
F (%)	58.47	39.33

Figure 2.1 The plasma concentration-time profiles of BHA after intravenous administration. Wild type and knockout mice were dosed intravenously with 25 mg/Kg of BHA. Data are expressed as mean ± SD, *n* = 3 or 4.

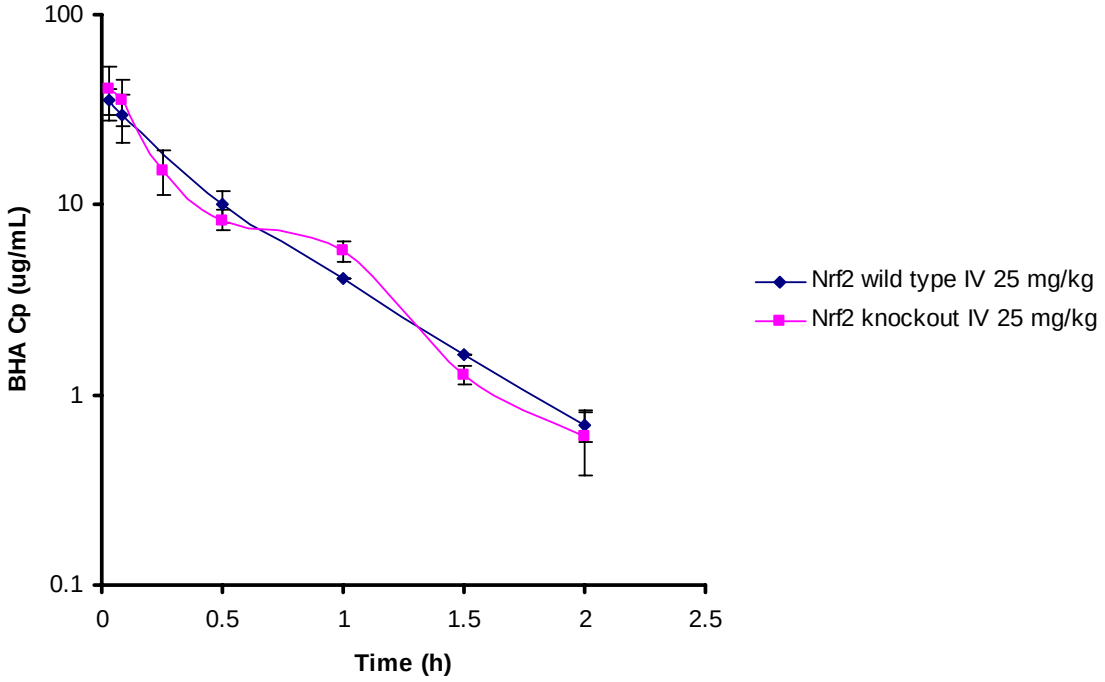

Figure 2.2 The plasma concentration-time profiles of DBM after oral administration. Wild type and knockout mice were dosed by oral gavage with 200 mg/kg of DBM. Data are expressed as mean ± SD, n = 3 or 4.

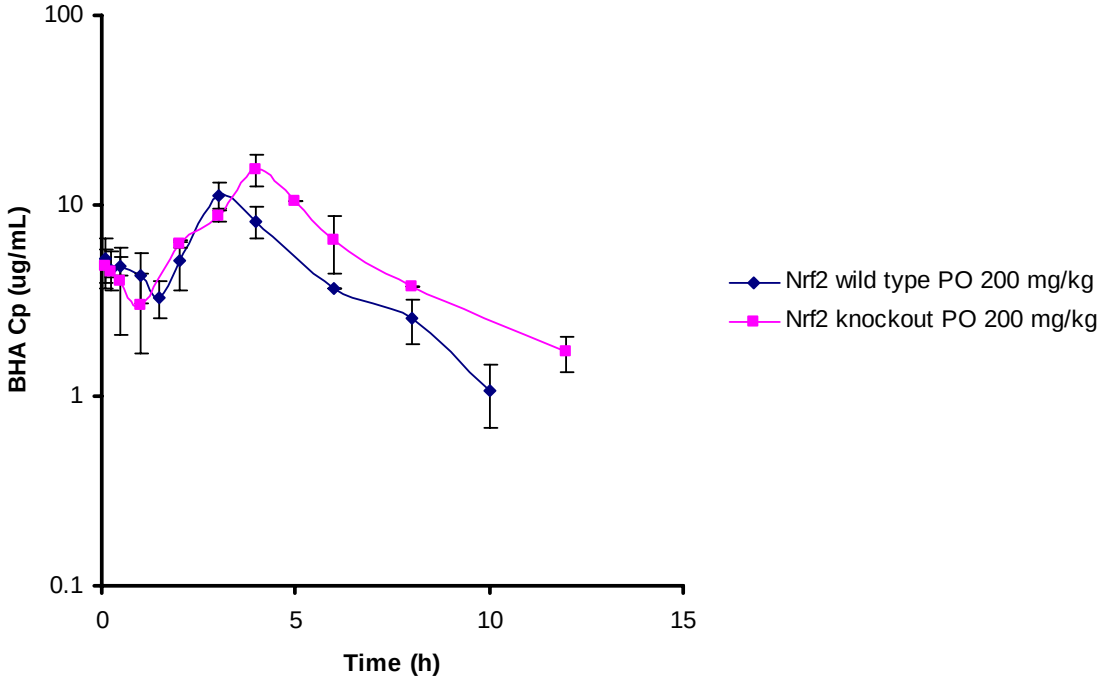

Figure 2.3 BHA plasma concentrations at early time points (from 2 mins to 1h) after i.v. administration. Data are expressed as mean ± SD, *n* = 3 or 4.

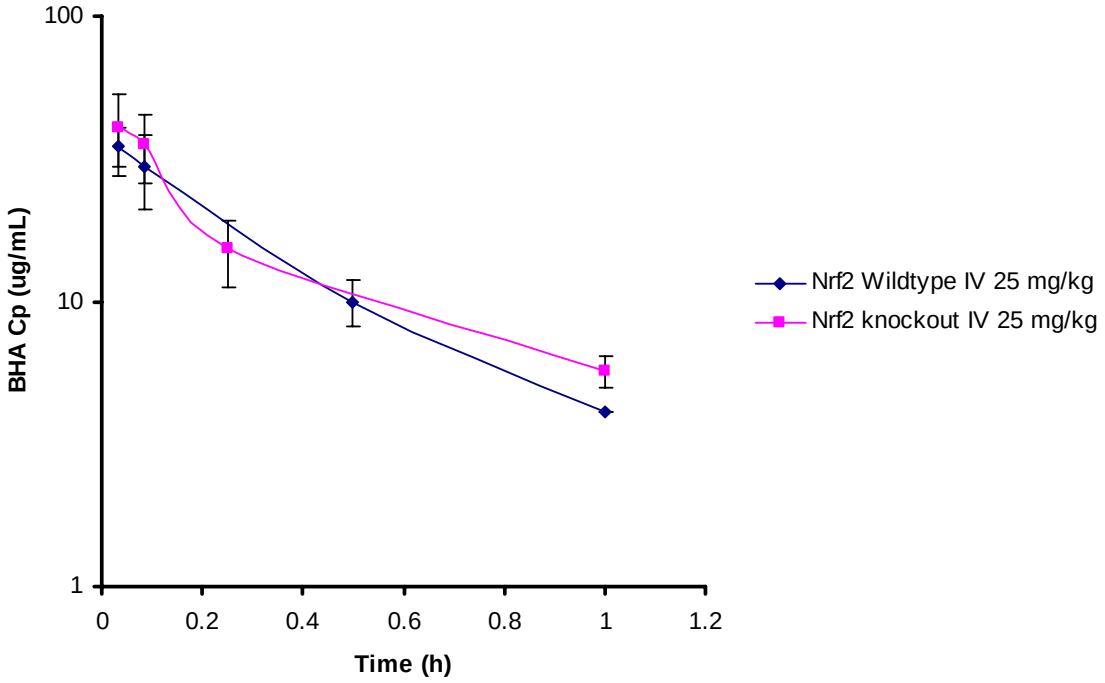

Figure 2.4 BHA plasma concentrations at early time points (from 5 mins to 1h) after oral administration. Data are expressed as mean ± SD, *n* = 3 or 4.

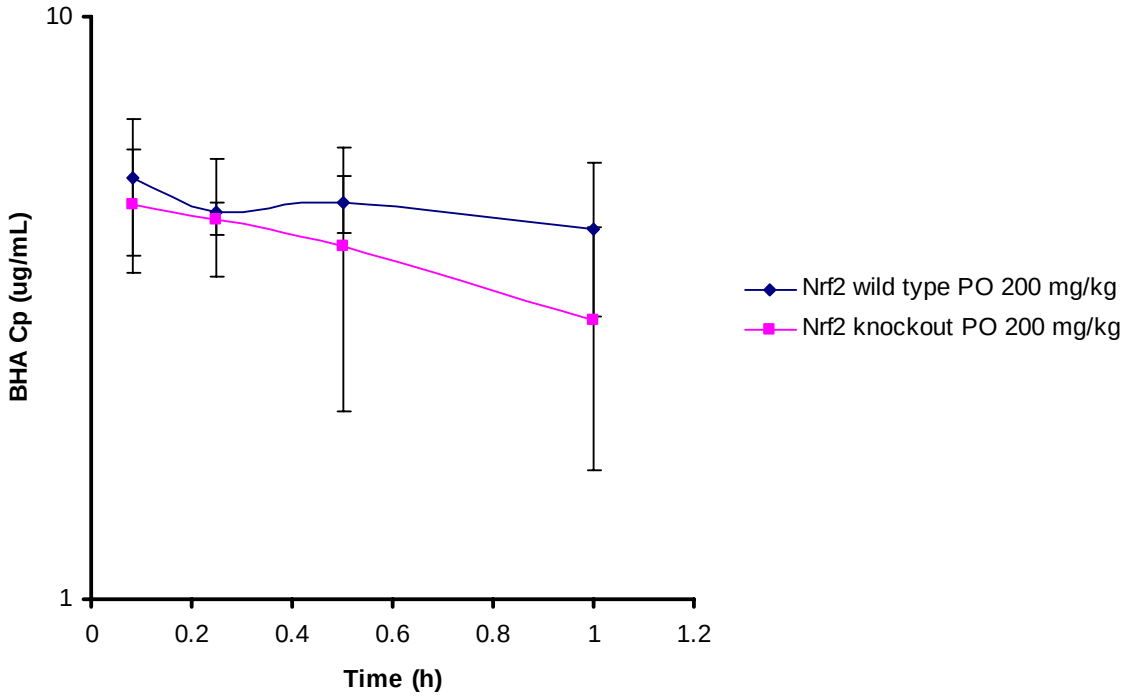

CHAPTER 3

Pharmacokinetics of Chemopreventive Compound Dibenzoylmethane in Nanoparticle Emulsion after Oral Administration

3.1 Introduction

Nanotechnology has become an integral part of the realm of drug delivery. Its integration was inevitable. The convenience and efficiency of combining the fields of medicine and therapeutic delivery with the growing universe of nanotechnology and nanoparticles were obvious. Although the cells themselves are larger than the usual size of a nanoparticle, the final targets of therapeutic drugs, i.e. the membrane protein complexes, membrane pores, organelles, ribosomes, chromosomes, and even DNA itself, themselves are in the range of nanometers (25). Thus it is no surprise that as the technology for nanoparticle manipulation advances, the usage of nanoparticles as drug carriers becomes more widespread. Nanotechnology's increasing popularity in the pharmaceutical field makes promises of more efficient drug delivery systems and subsequently, better health and life for humankind.

Dibenzoylmethane (DBM), a ß-diketone structural analog of curcumin, is a minor constituent of licorice. Previous studies have shown DBM to be capable to suppress the 7,12-dimethylbenz(2)anthracene (DMBA)-induced and estradiol (E_2)-induced mammary tumorgenesis and carcinogenesis both *in vivo* and *in vitro*. Studies show that DBM inhibits E_2-induced cell proliferation in both human breast cancer cells and mouse mammary glands through the E_2-ER-ERE dependent pathways. Some proposed mechanisms of DBM's involvement in prevention of tumorgenesis induced by DMBA

include its reduction of DMBA metabolism and the formation of DMBA-DNA adducts and its assistance in the elimination of many of DMBA's toxic metabolites through the induction Phase II detoxifying enzymes (26). It is strongly believed that DBM's chemopreventive ability derives from its ability to induce many Phase II detoxifying genes that include glutathione transferases and NAD(P)H: quinine reductase (27,28). In addition, both DBM and its derivatives have been used as sun-screening agents (29). A study using mouse models showed that DBM has the anticarcinogenic effects in TPA-induced skin inflammation/tumor promotion.

Previously, in a pharmacokinetics study done on Sprague-Dawley rats, we found that DBM had relatively low bioavailability of 13.6, 11.5, and 7.7% at 10, 20 and 250 mg/kg doses. The *ka* was 2.86 h^{-1}, which suggested that the absorption of DBM was relatively low with the vehicle (Cremophor El/tween-80/ethanol/water, 2:1:1:6 v/v) we used (Hong et al, accepted manuscript, 2008). In an effort to find a more effective drug delivery system in hopes of increasing the bioavailability of the DBM, we turned to nanotechnology and switched the vehicle to a nanoparticle drug carrier. Although the bioavailability of DBM in the former vehicle seemed decent in mice, we hope to further increase the exposure of DBM in mice following oral administration.

3.2 Materials and Methods

3.2.1 Chemicals

1,3-Diphenyl-1,3-propanedione (dibenzoylmethane, DBM,) and internal standard (I.S.) 1-(5-Chloro-2-hydroxy-4-methylphenyl)-3-phenyl-1,3-propanedione (CHMPP) were purchased from Sigma (St. Louis, MO, USA) at purity of more than 98%.

Acetonitrile and methanol were all HPLC grade from Fisher Scientific. Trifluoroacetic acid (TFA) was spectrophotometric grade (> 99%, Aldrich, WI, USA). Ethyl acetate was purchased from Sigma with purity of 99.9%. Other chemicals used in this study were all in analytical grade unless specified.

3.2.2 Preparation of DBM in nanoparticle vehicle

The components of the emulsion are DBM/tween 20/glycerol monooleate medium-chain triglycerides (MCT)/water (2:3:3:15:77 v/v). DBM was first dissolved in the MCT. Then the tween 20 and glycerol monooleate are dissolved in water. The MCT and the water mixture were mixed by stirring for ~ 1 min. After mixing, the crude emulsion is homogenized by high speed homogenizer (24000rpm) for ~1 min. Finally, the emulsion is passed through a high pressure homogenizer (1500 bar) for 10 cycles (70 nm). The average particle size was found to be 100 to 110 nm.

3.2.3 Animals and Dosing

Male Sprague-Dawley rats weighing 250-300 grams, implanted with a jugular vein cannuale were ordered from Hilltop Laboratory Animals (Scottdale, PA). C57BL/6J mice were purchased from Jackson Laboratory (Bar Harbor, ME, USA). The rats and mice were housed at the Animal Care Facility of Rutgers University, where they were acclimatized for at least three days with free access to food and water. The animals were fast overnight and given a dose of 250 mg/kg of DBM in the nanoparticle emulsion vehicle via oral gavage. Blood samples (300 μL) were collected at 30 min, 1, 1.5, 2, 4, 6, 8, 12, 24, 36h following DBM administration. The rats' blood samples were collected every twelve hours after 36h up to 96h. Plasma was separated immediately by centrifugation and stored at - 80°C until analysis.

3.2.4 HPLC analysis of DBM

Rat plasma concentrations of DBM were determined by a validated HPLC-UV detection method that we previously developed (30). Briefly, a 50 μL aliquot of the plasma samples was spiked with the internal standard (CHMPP) working solution and extracted twice with 200 μL ethyl acetate/methanol (95:5 v/v) solution. The organic layer was separated by centrifugation and evaporated to dryness under nitrogen gas at room temperature. The residue was reconstituted in 100 μL of acetonitrile/water (50:50 v/v) solution, and 20 μL was injected onto a HPLC column. Analyses were performed using a Shimadzu HPLC system at 4°C with a reverse phase column (Gemini^{TM} C18 column, 150 x 2.0 mm, 5-μm, Phenomenex, Torrance, CA USA) protected with a SecurityGuard^{TM} cartridge system (Phenomenex) and a 0.45-μm in-line filter. The binary gradient mobile phase (mobile phase A: water/methanol (80:20, v/v) with 0.1 % TFA and mobile phase B: acetonitrile with 0.1 % TFA) were pumped at the flow rate of 0.2 mL/min. The UV detector was set at a single wavelength of 335 nm. The Class-VP software version 7.1.1 (Shimadzu, MD USA) was used for instrument control and data analysis. The retention time for DBM and internal standard (CHMPP) were 21.4 and 24.0 min, respectively. The lower limit of quantification for DBM was 0.05 μg/mL and the linear calibration curves were obtained in the concentration ranges of 0.05-20 μg/mL. The intra- and inter-day precision and accuracy determination of quality control samples were below 15%.

3.2.5 Data Analysis:

The obtained DBM plasma concentration data was analyzed using WinNonlin 4.0 software (Pharsight, CA USA) to obtain pharmacokinetic parameters.

3.3 Results and Discussion

3.3.1 Pharmacokinetics of DBM in rats

DBM (Figure 3.1) is a minor constituent in licorice. It has been of interest in recent years, because studies have found it to possess potent anti-carcinogenesis effect. In our previous pharmacokinetics study, the bioavailability of DBM was relatively low. Using a nanoparticle delivery vehicle, we hope to increase the bioavailability and exposure of DBM after oral administration.

The mean concentration-time profile of DBM in the nanoparticle emulsion and old vehicle after oral administration of 250 mg/kg in rats is shown in Figure 3.2. The pharmacokinetics parameters determined by noncompartmental analysis following oral administration of DBM in the nanoparticle emulsion and old vehicle in rats are summarized in Table 3.1. Every pharmacokinetics parameters with the exception of T_{max} was increased by at least 1.38 fold. The AUC following oral administration was 94.16 ± 24.79 μg•hr/mL, which is a 3 fold increase from the AUC (31.89 ± 6.89 μg•hr/mL) of DBM after oral administration at 250 mg/kg with the old vehicle. The $t_{1/2}$ was found to be 31.12 ± 1.53 h, which is a 2.275 increase over the $t_{1/2}$ found after administration of the old formulation. The C_{max} (4.00 ± 1.07 μg/mL) increased 1.38 fold, MRT (18.02 ± 1.62 h) a 1.73 fold increase, and bioavailability (36.11%) increased a significant 4.68 fold. The T_{max} was lower in the rats after the oral administration of the nanoparticle emulsion compared to that found after oral administration with the old formulation, suggesting that the nanoparticle vehicle allows better absorption of DBM in rats. Taken altogether, the pharmacokinetics parameters suggest that DBM is better absorbed and not as quickly cleared when it is delivered in the nanoparticle emulsion than in the old delivery vehicle.

Plasma concentration of DBM could be detected up to 60 hours after oral administration with the nanoparticle emulsion. Our previous pharmacokinetics on DBM suggested that DBM does not follow linear pharmacokinetics when orally administrated. Its bioavailability decreases as dose increases. If these findings are true, then it is possible that the bioavailability of DBM will be even greater than 36.11% at lower doses.

In a study that used wild type Hepa1c1c7 cells derived from rodents, DBM was found to induce quinine-reductase (QR) activity two folds at a concentration of 1.9 μM. DBM's ability to induce phase II detoxifying enzymes and subsequently, inhibit carcinogen-induced tumorigenesis was evaluated on its ability to induce QR (26). The peak concentration of 4 μg/mL or 17.84 μM after oral administration of DBM in the nanaparticle emulsion at 250 mg/kg suggests that an oral dose of 250 mg/kg yields plasma concentration above the minimum concentration that is required to have therapeutic effects and that the 250 mg/kg is a therapeutic dose.

3.3.2 Pharmacokinetics of DBM in mice

The plasma concentration-time profile of DBM in the nanoparticle emulsion after oral administration of 250 mg/kg in mice is shown in Figure 3.3 The mean dose-normalized plasma concentration-time profile of DBM in the nanoparticle emulsion and old vehicle after oral administration of 250 mg/kg in mice is shown in Figure 3.4. The pharmacokinetics parameters determined by noncompartmental analysis following oral administration of DBM in the nanoparticle emulsion and old vehicle in mice are summarized in Table 3.2. Previously, we used a dose of 500 mg/kg in mice, because in our previous *Apc*$^{Min/+}$ mice study, we found 0.5 % DBM in diet could effectively regulate many cellular events which lead to tumorigenesis, we calculated it is approximately equal

to a dose of 500 mg/kg daily for a mouse with 30g of body weight (3). However, in this study, the mice were given an oral dose of 250 mg/kg. Not surprisingly, some of the pharmacokinetics parameters, such as C_{max} (13.65 ± 0.030 μg/mL) and AUC (48.91 ± 13.40 μg•hr/mL), after an oral administration of 250 mg/kg when compared to the corresponding ones (64.61 μg•hr/mL and 23.19 μg/mL, respectively) after dose of 500 mg/kg. The t_{max} seemed to have increased in mice after being orally administered with the nanoparticle emulsion (1 h) relative to the old formulation (15 min). This means the nanoparticle emulsion of DBM is being absorbed slower, not necessarily less, than the old formulation. Upon comparing the dose-normalized plasma concentration time profiles of the nanoparticle emulsion of DBM at 250 mg/kg and the old formulation of DBM at 500 mg/kg, it did seemed that the nanoparticle emulsion yielded a proportionally higher plasma concentrations in the mouse than the old formulation up to 12 hours after administration, suggesting that the nanoparticle emulsion is better absorbed in mice. The dose-normalized AUC values for oral dose of 250 mg/kg and 500 mg/kg were 0.196 and 0.129, which further indicates better absorption of DBM when it is suspended in the nanoparticle emulsion.

Interestingly enough, DBM was undetectable at the 36 hour time point in mice while at the same dose of 250 mg/kg, plasma concentrations of DBM were detectable up to 60 hours after administration. It seems that DBM is cleared faster in mice than in rats. Another observation made when comparing the two sets of pharmacokinetics parameters of the two animal models, we observed a higher exposure of DBM in rats than in mice when previously, mice had a higher exposure of DBM relative to rats. All these findings

seem to point out that the nanoparticle emulsion is more effective in increasing the absorption and exposure of DBM in rats than in mice.

Overall, using nanoparticle drug delivery system for DBM seems to be effective in increasing the absorption in both mice and rat models and increasing its exposure. With increasing interest in DBM as a valid chemopreventive agent, there is a growing necessity to address certain factors about its chemical and pharmacokinetics properties, such as its strong lipophilicity, which may in turn be a distributing to its low bioavailability and low *ka*. We propose a different drug delivery system, one that uses the nanotechnology in an effort to overcome the possible problem of DBM precipitating out of the drug delivery vehicle due to its insolubility in water and to increase the absorption of DBM. The results of this study indicate that the nanoparticle emulsion may be a promising way to deliver DBM into cells more efficiently.

Table 3.1 Pharmacokinetics parameters of DBM after oral administration in rats determined by Noncompartmental Analysis.

Dose (250 mg/Kg)	New Emulsion (n =3)	Old formulation (*n* = 3)
AUC (μg*hr/mL)	94.16 ± 24.79	31.89 ± 6.89
$t_{1/2}$ (hr)	31.12 ± 1.53	13.68 ± 3.77
T_{max} (hr)	1.67 ± 0.29	3.33 ± 1.15
C_{max} (μg/mL)	4.00 ± 1.07	2.88 ± 0.74
MRT (hr)	31.12 ± 1.54	18.02 ± 1.62
F (%)	36.11	7.72

Table 3.2 Pharmacokinetics parameters of DBM after oral administration in mice determined by Noncompartmental Analysis.

Dose (250 mg/Kg)	New Emulsion (n =2)	Old formulation (n=4)
AUC (μg*hr/mL)	48.91 ± 13.40	64.61
$t_{1/2}$ (hr)	2.47 ± 0.497	6.09
T_{max} (hr)	1 ± 0	0.25
C_{max} (μg/mL)	13.65 ± 0.030	23.19
MRT (hr)	3.92 ± 0.458	4.73

Figure 3.1 Chemical structure of DBM

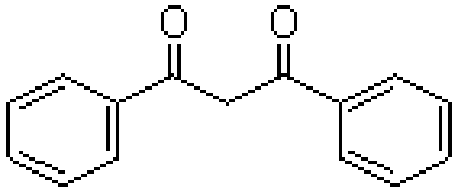

Figure 3.2 The mean concentration-time profile of DBM in the nanoparticle emulsion and old vehicle after oral administration of 250 mg/kg in rats. Mean ± SD, $n = 3$

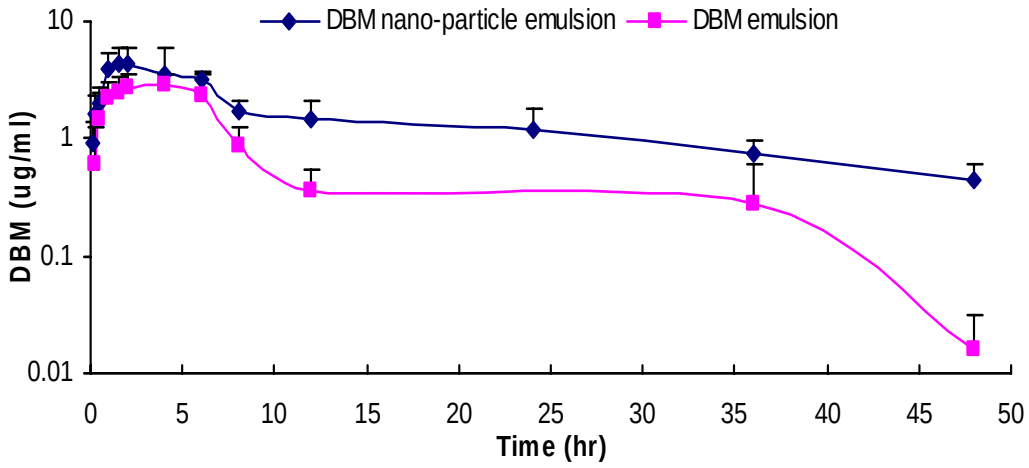

Figure 3.3 The plasma concentration-time profile of DBM in the nanoparticle emulsion after oral administration of 250 mg/kg in mice. Mean ± SD, $n = 2$

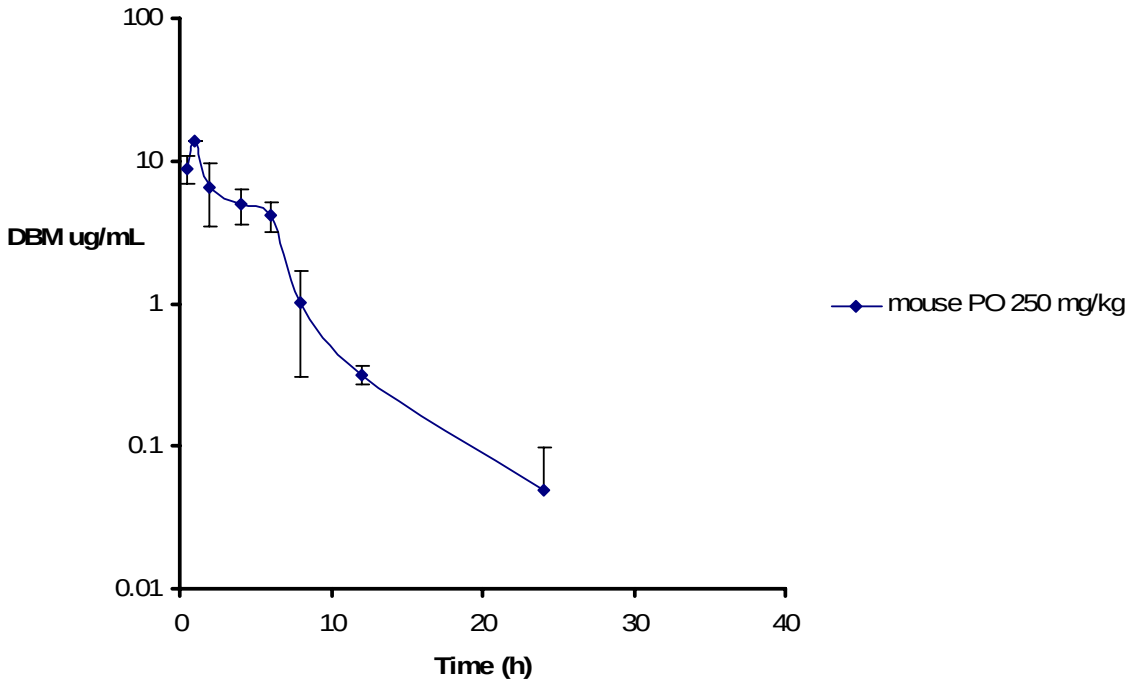

Figure 3.4 The mean dose-normalized plasma concentration-time profile of DBM in the nanoparticle emulsion and old vehicle after oral administration of 250 mg/kg in mice. Mean ± SD, *n* = 2 or 4

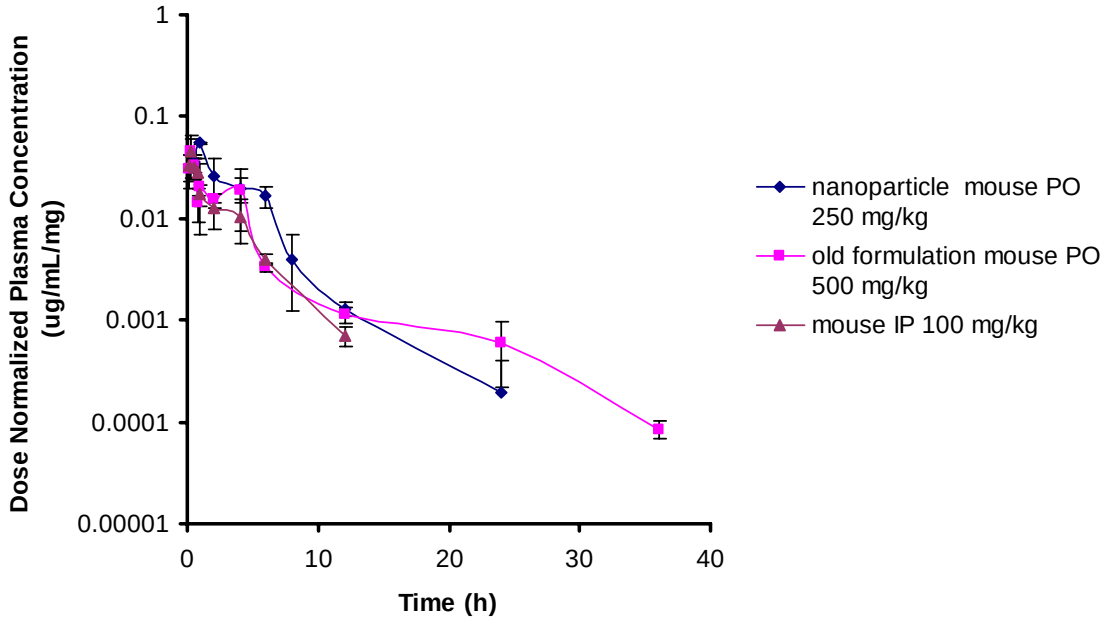

References

1. Kwon, K.H. *et al.* (2007) Cancer chemoprevention by phytochemicals: potential molecular targets, biomarkers and animal models. *Acta Pharmacol Sin*. **28**, 1409-21.
2. Yu, R. *et al.* (1997) Butylated hydroxyanisole and its metabolite tert-butylhydroquinone differentially regulate mitogen-activated protein kinases. The role of oxidative stress in the activation of mitogen-activated protein kinases by phenolic antioxidants. *J Biol Chem*. **272**, 28962-70.
3. Shen, G. *et al.* (2007) Chemoprevention of familial adenomatous polyposis by natural dietary compounds sulforaphane and dibenzoylmethane alone and in combination in ApcMin/+ mouse. *Cancer Res*. **67**, 9937-44.
4. Wattenberg, L.W. *et al.* (1979) Inhibitory effects of butylated hydroxyanisole on methylazoxymethanol acetate-induced neoplasia of the large intestine and on nicotinamide adenine dinucleotide-dependent alcohol dehydrogenase activity in mice. *J Natl Cancer Inst*. **63**, 219-22.
5. Hu, R. *et al.* (2006) In vivo pharmacokinetics, activation of MAPK signaling and induction of phase II/III drug metabolizing enzymes/transporters by cancer chemopreventive compound BHA in the mice. *Arch Pharm Res*. **29**, 911-20.
6. Nair, S. *et al.* (2006) Pharmacogenomics of phenolic antioxidant butylated hydroxyanisole (BHA) in the small intestine and liver of Nrf2 knockout and C57BL/6J mice. *Pharm Res*. **23**, 2621-37.
7. Ito, N. *et al.* (1983) Induction of papilloma in the forestomach of hamsters by butylated hydroxyanisole. *Gann*. **74**, 459-61.
8. Clayson, D.B. *et al.* (1990) The significance of induced forestomach tumors. *Annu Rev Pharmacol Toxicol*. **30**, 441-63.
9. Keum, Y.S. *et al.* (2006) Induction of heme oxygenase-1 (HO-1) and NAD[P]H: quinone oxidoreductase 1 (NQO1) by a phenolic antioxidant, butylated hydroxyanisole (BHA) and its metabolite, tert-butylhydroquinone (tBHQ) in primary-cultured human and rat hepatocytes. *Pharm Res*. **23**, 2586-94.
10. Anderson, M.W. *et al.* (1981) Inhibition in vivo of the formation of adducts between metabolites of benzo(a)pyrene and DNA by butylated hydroxyanisole. *Cancer Res*. **41**, 4309-15.
11. Yang, Z. *et al.* (2005) Preclinical pharmacokinetics of a novel HIV-1 attachment inhibitor BMS-378806 and prediction of its human pharmacokinetics. *Biopharm Drug Dispos*. **26**, 387-402.
12. Davies, B. *et al.* (1993) Physiological parameters in laboratory animals and humans. *Pharm Res*. **10**, 1093-5.
13. Granero, G.E. *et al.* (2008) Possibility of enterohepatic recycling of ketoprofen in dogs. *Int J Pharm*. **349**, 166-71.
14. Shen, G. *et al.* (2006) Modulation of nuclear factor E2-related factor 2-mediated gene expression in mice liver and small intestine by cancer chemopreventive agent curcumin. *Mol Cancer Ther*. **5**, 39-51.
15. Noda, S. *et al.* (2003) Gene expression of detoxifying enzymes in AhR and Nrf2 compound null mutant mouse. *Biochem Biophys Res Commun*. **303**, 105-11.

16. Hu, R. *et al.* (2006) Identification of Nrf2-regulated genes induced by chemopreventive isothiocyanate PEITC by oligonucleotide microarray. *Life Sci*. **79**, 1944-55.
17. McMahon, M. *et al.* (2001) The Cap'n'Collar basic leucine zipper transcription factor Nrf2 (NF-E2 p45-related factor 2) controls both constitutive and inducible expression of intestinal detoxification and glutathione biosynthetic enzymes. *Cancer Res*. **61**, 3299-307.
18. Tanaka, Y. *et al.* (2008) Coordinated induction of Nrf2 target genes protects against iron nitrilotriacetate (FeNTA)-induced nephrotoxicity. *Toxicol Appl Pharmacol*.
19. Barve, A. *et al.* (2008) Pharmacogenomic Profile of Soy Isoflavone Concentrate in the Prostate of Nrf2 Deficient and Wild-Type Mice. *J Pharm Sci*.
20. Fotheringham, A.P. *et al.* (1991) Age-associated changes in neuroaxonal transport in the hypothalamo-neurohypophysial system of the mouse. *Mech Ageing Dev*. **60**, 113-21.
21. Shen, G. *et al.* (2004) Regulation of Nrf2 transactivation domain activity. The differential effects of mitogen-activated protein kinase cascades and synergistic stimulatory effect of Raf and CREB-binding protein. *J Biol Chem*. **279**, 23052-60.
22. Lam, P. *et al.* (2005) Bile acid transport in sister of P-glycoprotein (ABCB11) knockout mice. *Biochemistry*. **44**, 12598-605.
23. Guo, W. *et al.* (2008) Enzymatic reduction and glutathione conjugation of benzoquinone ansamycin Hsp90 inhibitors: Relevance for toxicity and mechanism of action. *Drug Metab Dispos*.
24. Okusanya, O. *et al.* (2007) Compartmental pharmacokinetic analysis of oral amprenavir with secondary peaks. *Antimicrob Agents Chemother*. **51**, 1822-6.
25. Husseini, G.A. *et al.* (2008) Micelles and nanoparticles for ultrasonic drug and gene delivery. *Adv Drug Deliv Rev*. **60**, 1137-52.
26. Singletary, K. *et al.* (1998) Effect of the beta-diketones diferuloylmethane (curcumin) and dibenzoylmethane on rat mammary DNA adducts and tumors induced by 7,12-dimethylbenz[a]anthracene. *Carcinogenesis*. **19**, 1039-43.
27. Lin, C.C. *et al.* (2001) Inhibition by dietary dibenzoylmethane of mammary gland proliferation, formation of DMBA-DNA adducts in mammary glands, and mammary tumorigenesis in Sencar mice. *Cancer Lett*. **168**, 125-32.
28. Lin, C.C. *et al.* (2001) Mechanistic studies on the inhibitory action of dietary dibenzoylmethane, a beta-diketone analogue of curcumin, on 7,12-dimethylbenz[a]anthracene-induced mammary tumorigenesis. *Proc Natl Sci Counc Repub China B*. **25**, 158-65.
29. Huang, M.T. *et al.* (1998) Effect of dietary curcumin and dibenzoylmethane on formation of 7,12-dimethylbenz[a]anthracene-induced mammary tumors and lymphomas/leukemias in Sencar mice. *Carcinogenesis*. **19**, 1697-700.
30. Shen, G. *et al.* (2007) Development and validation of an HPLC method for the determination of dibenzoylmethane in rat plasma and its application to the pharmacokinetic study. *J Chromatogr B Analyt Technol Biomed Life Sci*. **852**, 56-61.